Available online at www.sciencedirect.com

ScienceDirect

Energy Procedia 80 (2015) 201 – 212

Energy Procedia

12th Deep Sea Offshore Wind R&D Conference, EERA DeepWind'2015

Modelling of MMC-HVDC Systems – An Overview

A. Beddard and M. Barnes*

Power Conversion Group, School of Electrical and Electronic Engineering, University of Manchester,Sackville Street Building, Manchester, M13 9PL, UK

Abstract

Modular Multilevel Converters (MMC) are presently the converter topology of choice for Voltage Source Converter High Voltage DC (VSC-HVDC) transmission schemes due to their very high efficiency. Accurate models of these complex MMC-HVDC systems are therefore required for research and development. There are numerous publications in this area; however these publications tend to focus on a particular component within the scheme, rather than the overall system. A key objective of this paper is to act as a guide for modelling MMC-HVDC systems by giving an overview of the process for developing a typical Multi-terminal (MT) MMC-HVDC (MTDC) model. The MTDC model developed in this paper is then employed to show the effect that selected MT control strategies can have on the MMC's arm currents.

Peer-review under responsibility of SINTEF Energi AS

Keywords: Modelling; MMC; VSC; HVDC; DC cables.

1. Introduction

The demand for Voltage Source Converter (VSC) High Voltage Direct Current (HVDC) transmission schemes has grown significantly in recent years. This growth is primarily due to the improvements in the voltage and power ratings of insulated gate bipolar transistors and a number of new VSC-HVDC applications such as the connection

* Antony Beddard: Tel.: +441613064798
E-mail address: Antony.Beddard@Manchester.ac.uk; Mike.Barnes@Manchester.ac.uk

Peer-review under responsibility of SINTEF Energi AS
doi:10.1016/j.egypro.2015.11.423

of large offshore windfarms.

Since its inception in 1997 and until 2010 all VSC-HVDC schemes employed two or three level VSCs [1]. In 2010, the Trans Bay cable project became the first VSC-HVDC scheme to use Modular Multi-level Converter (MMC) technology. The MMC has numerous benefits in comparison to two or three level VSCs; chief among these is reduced converter losses. Today, the main HVDC manufacturers offer a VSC-HVDC solution which is based on multi-level converter technology.

Detailed electromagnetic transient models are vital for these MMC-HVDC transmission schemes. There are a number of excellent publications in this area; however these publications tend to focus on a particular component within the scheme. One notable exception is the recently published 220 page CIGRÉ technical brochure, "Guide for the development of models for HVDC converters in a HVDC grid" [2]. The key contribution of this paper is to describe the main aspects of MMC-HVDC modelling in a compact and integrated manner. A detailed MTDC system model for the connection of offshore windfarms is developed and the model's structure, control systems and derivation of parameters are described along with an outline of the different modelling options for MMCs and HVDC cables.

Numerous studies have been carried out to assess the performance of MTDC control strategies [3-5]. These studies have however employed simplified MTDC system models, which cannot always accurately represent the MMC dynamics and are unable to simulate the internal MMC quantities which are critical to ensuring that the converter is operating within safe limits. An example study using the detailed model developed in this paper is therefore carried out to show the impact that MTDC control strategies can have on the MMC's arm currents.

2. MMC-HVDC

Figure 1 shows a diagram of a MT MMC-HVDC system which is based on a sub-section of a potential scenario outlined in the UK National Grid's Offshore Development and Information Statement (ODIS) [6]. The main circuit parameters for this system are based on the information given in ODIS for the connection of a typical Round 3 windfarm in the UK. A table of key parameters for the system is given in the appendix.

2.1. MMC

The main component of MMC-HVDC systems are the converters. There are several types of MMC, including but not limited to: Half-bridge (HB), Full-bridge (FB) and Alternate Arm Converter (AAC) [7]. The FB-MMC and the AAC are referred to as fault blocking converters as they are able to block the current flowing through the converter in the event of a DC side fault. This can be particularly useful for HVDC schemes employing overhead transmission lines, however for HVDC grids using cables, a DC side fault is likely to be permanent and hence the need for fault blocking converters is not yet apparent. Furthermore, the HB-MMC is the only type of MMC which is commercially in operation. Considering that the majority of proposed MTDC systems are dominated by submarine cables, this paper focuses on the HB-MMC.

The basic structure of a three-phase HB-MMC is shown in Figure 2. Each leg of the converter consists of two converter arms which contain a number of Sub-Modules (SMs), and a reactor, L_{arm}, connected in series. Each SM contains a two-level HB converter with two IGBTs and a parallel capacitor. The module is also equipped with a bypass switch to remove the module from the circuit in the event that an IGBT fails, and a thyristor, to protect the lower diode from overcurrent in the case of a DC side fault. The bypass switch and thyristor are, however, typically omitted for most studies.

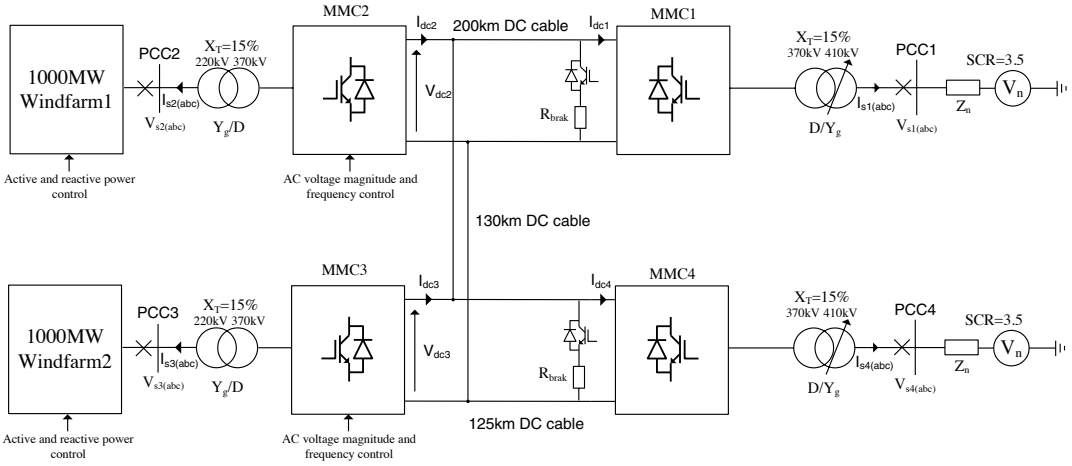

Figure 1: MT MMC-HVDC system model

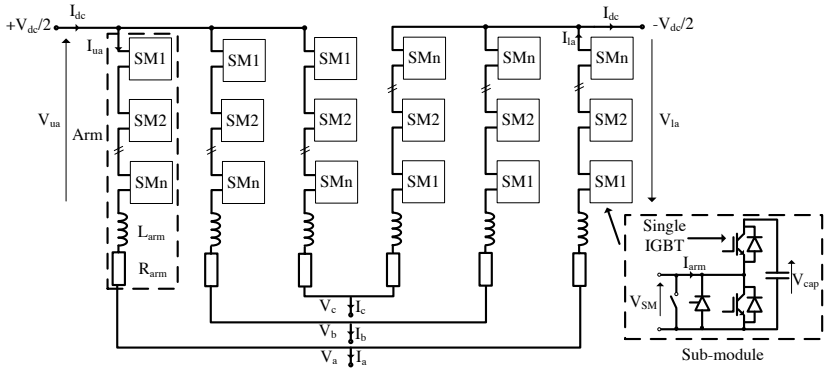

Figure 2: Three-phase HB-MMC

The SM terminal voltage, V_{SM}, is effectively equal to the SM capacitor voltage, V_{cap}, when the upper IGBT is switched-on and the lower IGBT is switched-off. The capacitor will charge or discharge depending upon the arm current direction. With the upper IGBT switched-off and the lower IGBT switched-on, the SM capacitor is bypassed and hence V_{SM} is effectively at zero volts. Each arm in the converter therefore acts like a controllable voltage source, with the smallest voltage change being equal to the SM capacitor voltage. The converter output voltages, $V_{(a,b,c)}$, are effectively controlled by varying their respective upper and lower arm voltages, $V_{u(a,b,c)}$ and $V_{l(a,b,c)}$ as described by equation (1) for phase A [8].

$$V_a = \frac{V_{la} - V_{ua}}{2} - \frac{L_{arm}}{2}\frac{dI_a}{dt} - \frac{R_{arm}}{2} I_a \qquad (1)$$

The number of discrete voltage levels the MMC is able to produce is dependent upon the number of SMs in the converter arms. As the number of SMs increase, the harmonic content of the output waveform decreases but the computational efficiency of the MMC converter model also decreases. Commercial MMC-HVDC schemes contain hundreds of SMs per converter arm [9]. The primary reason that such a large number of SMs per converter arm are required is to reduce the voltage stress across each SM to a few kV, it is however possible to use significantly less SMs and still not require AC filters. Determining the number of converter levels to model is therefore typically a

compromise between harmonic content of the output waveforms and the computational efficiency of the model. In our studies a 31-level MMC was found to offer a good compromise by meeting the IEEE519 harmonic voltage limits without having a significant impact on the simulation time.

The choice of the SM capacitance value, C_{SM}, is a trade-off between the SM capacitor ripple voltage and the size of the capacitor. A capacitance value which gives a SM voltage ripple in the range of ±5% is considered to be a good compromise [10]. According to [10] 30-40kJ of stored energy per MVA of converter rating is sufficient to give a ripple voltage of 10% (±5%). Alternatively the analytical approach proposed by Marquardt et al. in [11] can be used to calculate the approximate SM capacitance required to give an acceptable ripple voltage for a given converter rating.

The converter arm currents consist of three main components as given by equation (2) for phase A. The circulating current, I_{circ}, is due to the unequal DC voltages generated by the three converter legs. The circulating current is a negative sequence (a-c-b) current at double the fundamental frequency, which distorts the arm currents and increases converter losses [12].

$$I_{ua} = \frac{I_{dc}}{3} + \frac{I_a}{2} + I_{circ} \qquad I_{la} = \frac{I_{dc}}{3} - \frac{I_a}{2} + I_{circ} \tag{2}$$

The limb reactors, also known as converter reactors and arm reactors, which are labelled L_{arm} in Figure 2, have two key functions. The first function is to suppress the circulating currents between the legs of the converter and the second function is to reduce the effects of faults both internal and external to the converter. By appropriately dimensioning the limb reactors, the circulating currents can be reduced to low levels and the fault current rate of rise through the converter can be limited to an acceptable value. As the size of the limb reactor increases, the circulating current and the rate of rise of arm current in the event of a DC side fault decreases.

According to [13], the Siemens HVDC Plus MMC converter reactors limit the fault current to tens of amps per microsecond even for the most critical fault conditions, such as a short-circuit between the DC terminals of the converter. This allows the IGBTs in the MMC to be turned-off at non critical current levels. A minimum value of limb reactance to ensure that the arm current does not exceed 20A/μs for the worst case scenario is therefore a good starting point. The limb reactance can then be increased further as a compromise between the size of the reactor and the magnitude of circulating current. The circulating current can also be suppressed by converter control action or through filter circuits [10]. For our work a 45mH (0.1p.u.) limb reactor used in conjunction with a Circulating Current Suppressing Controller (CCSC) was found to offer a good level of performance.

There are many different techniques for modelling a MMC [14-16]. These range from very detailed semi-conductor physics based models which are too complex to model a full MMC, to very simple power flow models. The accuracy and simulation speed of a wide range of MMC models have been compared in numerous publications [14, 15, 17, 18]. Average Value Models (AVMs) are commonly used for modelling MMCs in MTDC systems as their overall accuracy is sufficient for many studies and they are significantly more computational efficient than the other more detailed models [14]. However, AVMs are unable to simulate the MMC arm currents and SM capacitor voltages, which are critical to ensuring that the converter is operating within safe limits during transient events.

Three of the leading detailed modelling techniques which are able to simulate the arm currents and SM capacitor voltages were compared in terms of their accuracy and simulation speed in [18]. These models are referred to as the Traditional Detailed Model (TDM), Detailed Equivalent Model (DEM) and the Accelerated Model (AM). Figure 3 shows the simulation times for a 16, 31 and 61 level MMC using the three modelling techniques with a 20μs time-step for a 5s simulation in PSCAD X4. The simulations were conducted on a computer with a 2.5-GHz Intel core iq7 processor and 8 GB of RAM. This figure shows that the DEM is at least two times faster than the AM and ten times faster than the TDM for a 31-level MMC. The results from [18] also shown that DEM was generally more accurate than the AM and offered a very similar level of accuracy to the

TDM, which was the benchmark model for the study. The DEM was therefore selected for this work.

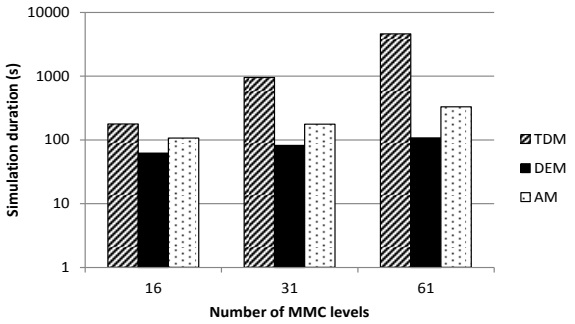

Figure 3: Simulation times of the three models for different MMC levels.

2.2. HVDC cable

A submarine HVDC cable, which is normally one of, if not, the most expensive component in a VSC-HVDC scheme is complex and consists of many concentric layers, which complicates its modelling as shown in Figure 4 [19]. The current carrying conductor may be made of copper or aluminium and the choice is normally project specific. The insulation layer provides an effective potential barrier between the conductor and the metallic screen/sheath. In VSC-HVDC schemes the insulation is typically XLPE because it is less expensive and more robust in comparison to mass-impregnated cables [20]. The conductor screen and insulation screen are required to protect the insulation from ridges/grooves which could be caused by extruding the insulation directly onto the conductor [21]. Any ridges/grooves in the insulation could result in an enhanced localised electric field stress which would reduce the dielectric strength of the insulation. The metallic screen/sheath contains the electric field within the cable as well as carrying fault current to earth [22]. Longitudinal water sealing is achieved by applying swelling tape, which also absorbs humidity diffusing into the cable [21, 23]. The inner jacket provides mechanical and corrosion protection and the armour provides mechanical protection against impacts and abrasions [19]. The armour usually has a zinc and bitumen coating to protect against corrosion. The outer cover is the final layer of the cable and prevents the zinc and bitumen coating from scratches which damage their anti-corrosion protection.

There are several types of cable model commercially available. Lumped parameter models are the simplest type of models used to represent cables. These models typically lump the cable's resistance, inductance, capacitance and shunt conductance together to form one or more PI/T-sections. The Bergeron model represents the distributed nature of the cable's inductance and capacitance with the resistance lumped together and split between each end of the cable (25% each end) and the middle of the cable (50%). Frequency dependent models represent the cable as a distributed RLC model, which includes the frequency dependency of all parameters. This type of model requires the cable's geometry and material properties to be known. There are two frequency dependent models available in PSCAD; the Frequency Dependent Mode Model (FDMM) and the Frequency Dependent Phase Model (FDPM), which are typical of advanced cable models. The key difference between the two models is that the phase model accounts for the frequency dependent coupling in the cable whereas the mode model does not. Furthermore, the phase model is able to produce the cable's exact DC response rather than a best approximation.

In [24] a coupled equivalent PI model, Bergeron model, FDMM and FDPM were compared in terms of accuracy and simulation speed for a variety of studies using the MTDC system shown in Figure 1. The results shown that choice of cable model can have a significant impact on the overall model's response for typical VSC-HVDC studies. The result also shown that the computational efficiency of the Bergeron, FDMM and FDPM were very similar while the use of coupled equivalent model resulted in a significantly longer simulation time. It is for these reasons that the FDPM, which is the most accurate model, is used for this work.

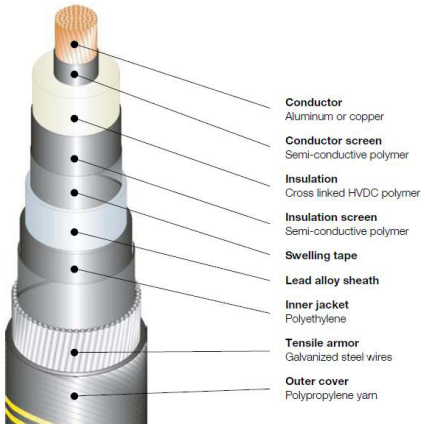

Figure 4: Image of a HVDC submarine cable, courtesy of ABB [19]

In the absence of publically available data for a commercial HVDC cable, the geometric and material properties for the layers of the cable, which can be represented in the FDPM cable model, were estimated for a 300kV 1GW cable DC-XLPE cable in [24]. These parameters are given in the appendix of this paper. It should be noted that a 300kV DC-XLPE cable will typically have a shunt conductance value of less than $1x10^{-12}$S/m [24, 25], however using such a smaller value of shunt conductance for the FDPM could result in passivity violations. The user should therefore take care when selecting a shunt conductance value for the model.

2.3. Dynamic braking system

A Dynamic Braking System (DBS), also commonly referred to as a DC chopper are typically employed for HVDC systems which are connected to windfarms. The main function of the DBS is to regulate the DC voltage by dissipating the surplus energy in the system which can arise when the VSC(s) are unable to export all of the wind power on the system. A DBS can be modelled as simply as voltage dependent current source [26], or as a power electronic switch connected in series with resistor for a more detailed representation. The basic control strategy for a DBS is to turn-on the IGBT valve once the DC voltage has exceeded a particular threshold and turn it off once the DC has returned below a specific threshold [27], however more complex strategies can be adopted [28]. A DBS could also be used to assist the surge arrestors in limiting transient DC over-voltages. The DBSs used is in the system for this work employ the basic upper and lower threshold control and there are designed to limit the maximum DC voltage to 1.2p.u using a 500Ω resistor.

2.4. HVDC breakers

In the absence of HVDC circuit breakers, a single DC cable fault can force an entire DC grid to be de-energized in order to isolate the faulty cable, which is likely to lead to large HVDC grids being technically and commercially unviable. Hybrid circuit breakers are currently seen as the most promising breaker topology with a number of HVDC manufacturers developing this type of breaker due to their low on-state losses and fast interruption speed [29-31]. HVDC circuit breakers are not modelled for this work, however some general modelling guidelines are given in [2] .

2.5. Converter transformer, onshore AC system and offshore AC system

VSC-HVDC systems are presently symmetrical monopoles and typically use a conventional AC transformer. The winding configuration of the converter transformer used in this work is delta/star, with the delta winding on the converter side of the transformer as is the case for the Trans Bay Cable project [32]. A tap-changer is employed

on the star winding of the transformers located onshore to assist with voltage regulation. In EMT software packages, transformers are normally modelled using the classical approach or using a Unified Magnetic Equivalent Circuit (UMEC) model [33]. The key difference between the models is that the UMEC model considers the coupling between the windings of the same phase and of different phases [33]. Both transformer models are able to represent the transformer's saturation characteristic, which is important for some studies [34]. Obtaining sufficient data from the public domain to get an accurate saturation characteristic for a large power transformer can however be challenging. In light of the limited public domain data and in common with many other studies, the transformers in this work are modelled using the classical approach without the saturation characteristic enabled. The need for further work in this area is however acknowledged. The transformer leakage reactance is set to 0.15p.u. with copper losses of 0.005p.u., which are typical values for a power transformer [35].

The representation of AC systems varies depending upon the type of software package being used and the type of study being investigated [34]. Fundamental frequency studies carried out in packages such as DigSilent Power Factory tend to use detailed models of the AC system and simplified models of the HVDC system. EMT type studies being investigated in software packages such as PSCAD typically use simplified models of the AC system and detailed models of the HVDC system. Hybrid simulation packages can also be used, which enable detailed representation of the HVDC system and associated AC systems without impractical simulation times, however hybrid simulation is not yet commonplace [2]. Further work in this area would be useful to give greater guidance on the necessary level of fidelity of AC systems for the range of MMC-HVDC studies. The focus of this work is on the HVDC system so a very simple, commonly used, AC system model of a voltage source connected in series with an impedance is employed. The strength of an AC system is often characterised by its Short-circuit Ratio (SCR). An AC system with a SCR greater than three is defined as strong [34]. The SCR of the AC system in this model is selected to be relatively strong with a SCR of 3.5.

Round 3 windfarms in the UK, as presently proposed, are typically rated at 1GW for HVDC connections. A 1GW offshore windfarm would typically contain 200 wind turbines based on a 5MW turbine design. The wind turbines are typically connected to two 500MW AC collector stations where the voltage is increased from 33kV to 220kV for transmission to the offshore converter. A range of modelling approaches exists for windfarms [36-38]. Modelling such a large number of wind turbines in detail in EMT simulation packages is very computational intensive and unnecessary for some VSC-HVDC studies. Simplified windfarm models are therefore often employed [39]. However, more work is required to give better guidance on the level of windfarm model fidelity required for the different MMC-HVDC studies. For this work a very simple windfarm model consisting of a three phase voltage connected to a 33kV/220kV transformer is employed since the HVDC link is the focus. The three phase voltage is controlled using a dq controller to inject active power into the offshore MMCs. The wind turbine, generator and back-to-back converter are represented as a first order transfer function with a time constant. The time constant for a large commercial wind turbine is expected to be around 15s, however such a large time constant would require very lengthy simulation times and for illustration it is therefore reduced to 0.15s which is suitable for this model.

2.6. Control systems

For a VSC-HVDC scheme which connects two active networks, one converter controls active power or frequency and the other converter controls the DC link voltage. The converters at each end of the link are capable of controlling reactive power or the AC voltage at the Point of Common Coupling (PCC). For a point-to-point VSC-HVDC link which is employed for the connection of a offshore windfarm, the offshore MMC's function is regulate the offshore AC network's voltage and frequency [39] and onshore MMC's function is to regulate the DC voltage. In a MTDC network, such as the one shown in Figure 1, the offshore converters can be controlled in the same way as they are in a point-to-point link. The regulation of the DC link voltage for a MTDC system is however more complex than in a point-to-point link.

A basic diagram showing an example control system for a MMC is shown in Figure 5.

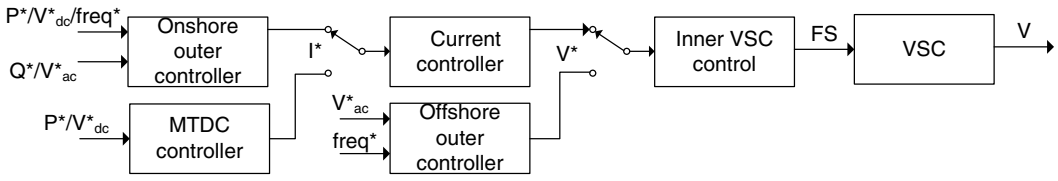

Figure 5: MMC control system basic overview

The internal MMC controls typically include a modulation controller, a Capacitor Balancing Controller (CBC) and a Circulating Current Suppressing Controller (CCSC). The modulation controller's function is to translate the voltage set-points into Firing Signals (FS) for the MMC to obtain the desired output voltage magnitude and phase. A number of modulation methods have been proposed for MMCs [40, 41]. The Nearest Level Controller (NLC) method produces waveforms with an acceptable amount of harmonic content when a suitable number of MMC levels are employed. It is the least computational complex method of the aforementioned techniques and, thus, is used for the model in this paper. The CBC ensures that the energy variation in each converter arm is shared equally between the submodules within that arm. The CBC method proposed in [11] has formed the basis of many of the capacitor balancing controllers for VSC–HVDC MMCs [15, 42, 43]. The CBC employed for this work is also based on this method. The CCSC minimises the circulating currents within the MMC by manipulating the voltage reference to upper and lower converter arms. The CCSC employed in this work is based on [12].

Unlike the internal MMC controls, the current controller, outer controllers and MTDC controllers are not VSC topology specific. The current controller is typically a fast feedback controller, which produces a voltage reference for the MMC based upon the current set-point from the outer feedback controller. Positive sequence dq control which is commonly used for VSCs is employed for the MMC in this work because it can limit the phase currents under balanced operating conditions and provide a faster response than direct control of the voltage magnitude and phase. More complex controllers such as negative sequence dq control and proportional resonance control have also been proposed for converters due to their ability to limit currents under unbalanced conditions [44].

The outer controllers are normally proportional-integral controllers which are typically tuned for a bandwidth of at least 6-10 times slower than the current controller. The outer controllers manipulate the d-axis current set-point to obtain the active power (P*) or DC voltage (V^*_{dc}) or frequency (freq*) set-point, and the q-axis current set-point to obtain the reactive power (Q*) or AC voltage magnitude (V^*_{ac}) set-point. The AC voltage magnitude and frequency for the offshore network can be controlled with or without an inner current loop [39, 45]. In this work, the voltage magnitude is set by controlling the d-axis voltage without an inner current loop and using a voltage controlled oscillator to set the angle based on the frequency set-point for the offshore network. This approach was found to offer good stability, however the arm currents cannot be limited for offshore AC network fault without supplementary control.

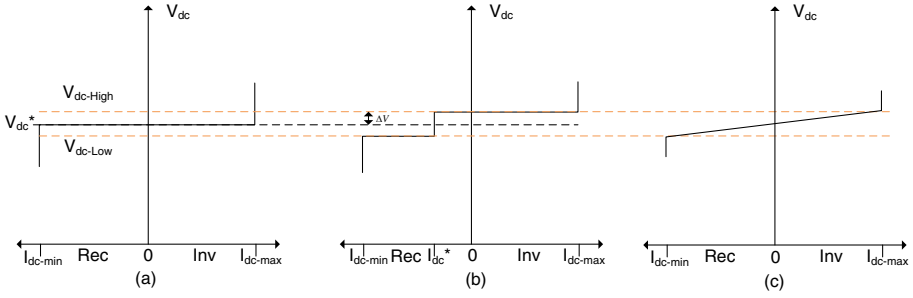

Figure 6: Typical MT control DC voltage/current characteristics: (a) slack bus; (b) voltage margin; (c) droop

A review of MTDC control methods is given in [3, 46]. Generally speaking these methods can be categorised as centralised DC slack bus, voltage margin control, droop control or a combination of the aforementioned control methods. Typical DC voltage/current characteristics for a converter employing the different MT control methods are shown in Figure 6. Employing a centralised DC slack bus means that one of converters operates in DC voltage control and must import/export the necessary active power in order to regulate the DC voltage. However, if the required active power is outside of the DC slack bus converter's capability then it will no longer be able to control the DC voltage, resulting in grid instability. An alternative is to operate another converter in voltage margin control. The converter employing voltage margin control operates as a constant power controller and transitions to DC voltage control if the DC voltage violates pre-set limits. Voltage margin control therefore improves the reliability of the system in comparison to a centralised DC slack bus. There are however a number of limitations when employing voltage margin control, such as the inability of more than one converter to participate in DC voltage regulation simultaneously. In droop control more than one converter is able to participate in regulating the DC voltage and therefore the burden of continuously balancing the system's power flow is not placed upon a single converter. Converters operating in droop control respond to changes in the DC voltage/current by modifying the d-axis current directly or indirectly via a DC voltage controller or an active power controller in accordance with the droop characteristic. The droop controllers used in this work modify the d-axis current set-point directly in accordance with the change in DC voltage.

There are several publications which describe the mathematical representation and tuning techniques for typical VSC controls [4, 47]. For this work the current controllers and power controllers were tuned for a first order response with a bandwidth of 320Hz and 30Hz respectively, and the DC voltage controller was tuned as a reduced 2^{nd} order system with an approximate bandwidth and damping ratio of 20Hz and 0.7 respectively. The parameters for all the controllers used in this model are given in the appendix.

3. Example Study – MT control impact on MMC arm currents

The MTDC model developed in this paper is used in the section to show the effect that MT control strategies can have on the MMC arm currents, which are critical to ensure safe operation of the MMC. The centralised DC slack bus control, voltage margin control and droop control methods are investigated in this paper with the control permutations shown in Table 1. Windfarm 1 and windfarm 2 are ordered to inject 500MW and 1GW respectively. A three-phase symmetrical fault is applied at PCC1 (Figure 1) for 140ms starting at 2s. MMC1 is therefore unable to export any significant quantity of active power during the fault. The phase A upper arm current waveforms after the AC fault is cleared are shown on the same graph in Figure 7. This figure shows the significant impact that the MTDC control methods can have on the converter's arm currents and highlights the importance of detailed MMC models for plant design even when comparing MT control methods. It should be noted that pre-fault arm currents for MMC1 when operating in droop control were approximately 25% less than the DC slack case and voltage margin case due to the near equal power sharing between the onshore converters.

Table 1: Control methods investigated

Control Method	MMC1 control mode	MMC4 control mode	Comments
Centralised DC slack bus	DC voltage & AC voltage magnitude	Active power & reactive power	P*=500MW
Voltage margin control	DC voltage & AC voltage magnitude	Voltage margin & reactive power	$V_{dc\text{-}High}$=620kV $V_{dc\text{-}Low}$=580kV
Droop control	Standard droop & AC voltage magnitude	Standard droop & reactive power	Droop gain =- 0.1

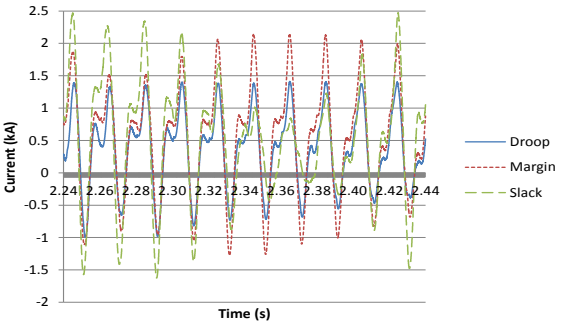

Figure 7: Impact of MTDC control methods on the upper arm current for phase A of MMC1 for a three-phase to ground fault

4. Conclusion

This paper has described the modelling process for a MT MMC-HVDC system, including the structure of the system, determining the value of key parameters, the different modelling techniques available and the numerous control functions which are required. Its key contribution is that the main aspects of MMC-HVDC modelling have been brought together and described in a compact and integrated manner. The paper also highlights areas of further research, especially the need for more detailed publications on the overall MMC-HVDC system fidelity required with the connected AC systems. Finally, the MT MMC-HVDC model developed in this paper is used to show how MT control strategies can impact on the MMC arm currents.

Acknowledgements

This work was supported by the UK Engineering and Physical Sciences Research Council (EPSRC) through grant EPSRC Project EP/L014106/1 Supergen Wind Hub. The authors would also like to thank Dr Robin Preece and Mr Wenyuan Wang for their useful discussions.

Appendix A. System parameters

Table 2: Key parameters for MTDC system

Component	Parameter	Symbol	Value
Main circuit	Active power rating	P	1000MW
	Reactive power rating	Q	±330MVAr
	DC voltage	V_{dc}	600kV
	Number of levels	NL	31
	Number of SMs per arm	n	30
MMC	SM capacitance	C_{SM}	1150μF
	Arm resistance	R_{arm}	0.9Ω
	Arm inductance	L_{arm}	0.045H
	Leakage reactance	X_T	0.15p.u.
Onshore MMC transformer	Star Primary winding voltage, L-L	V_{Tp}	370kV
	Delta Secondary winding voltage, L-L	V_{Ts}	410kV
	Apparent power base	S_{base}	1000MVA
Onshore AC system	Network voltage, L-L	V_n	400kV
	Network resistance	R_n	2.28Ω
	Network inductance	L_n	0.145H
MMC power controllers	Proportional gain	K_p	0.000208
	Integral time constant	T_i	2.387
MMC DC voltage controller	Proportional gain	K_p	0.0269

AC voltage controllers	Integral time constant	T_i	0.413
	Proportional gain	K_p	0.000208
	Integral time constant	T_i	2.39
MMC current controller	Proportional gain	K_p	175
	Integral time constant	T_i	0.000442
CCSC	Proportional gain	K_p	8.48
	Integral time constant	T_i	0.00589
Windfarm transformer	Leakage reactance	X_T	0.15p.u.
	Star Primary winding voltage, L-L	V_{Tp}	33kV
	Star Secondary winding voltage, L-L	V_{Ts}	220kV
Windfarm power controller	Proportional gain	K_p	0.00246
	Integral time constant	T_i	0.645
	Windfarm time constant	τ_w	0.15s
Windfarm current controller	Proportional gain	K_p	0.327
	Integral time constant	T_i	0.29
Offshore MMC voltage controller	Proportional gain	K_p	0.5
	Integral time constant	T_i	0.005
	Frequency	freq	50Hz
Offshore MMC transformer	Leakage reactance	X_T	0.15p.u.
	Star Primary winding voltage, L-L	V_{Tp}	370kV
	Delta Secondary winding voltage, L-L	V_{Ts}	220kV

Table 3: Data for a 300kV 1GW submarine HVDC cable [24]

Layer	**Material**	**Radial Thickness (mm)**	**Resistivity (Ω/m)**	**Relative Permittivity**	**Relative Permeability**
Conductor	Stranded Copper	24.9	$2.2\text{x}10^{-8*}$	1	1
Conductor screen	Semi-conductive polymer	1	-	-	-
Insulation	XLPE	18	-	2.5	1
Insulator screen	Semi-conductive polymer	1	-	-	-
Sheath	Lead	3	$2.2\text{x}10^{-7}$	1	1
Inner Jacket	Polyethylene	5	-	2.3	1
Armour	Steel	5	$1.8\text{x}10^{-7}$	1	10
Outer cover	Polypropylene	4	-	1.5	1
Sea-return	Sea water/air	-	1	-	-

*Copper resistivity is typically given as $1.68*10^{-8}\Omega$/m. It has been increased for the cable model in PSCAD due to the stranded nature of the cable which cannot be taken into account directly in PSCAD.

References

[1] M. Barnes and A. Beddard, "Voltage Source Converter HVDC Links – The state of the Art and Issues Going Forward," *Energy Procedia,* pp. 108-122, 2012.

[2] Cigre WG B4-57, "Guide for the Development of Models for HVDC Converters in a HVDC Grid," *WG Brochure,* 2014.

[3] W. Wang, M. Barnes, and O. Marjanovic, "Droop control modelling and analysis of multi-terminal VSC-HVDC for offshore wind farms," in *AC and DC Power Transmission (ACDC 2012), 10th IET International Conference on*, 2012, pp. 1-6.

[4] T. M. Haileselassie, M. Molinas, and T. Undeland, "Multi-terminal VSC-HVDC system for integration of offshore wind farms and green electrification of platforms in the North Sea," *Nordic Workshop on Power and Industrial Electronics, Espoo, Finland,* 2008.

[5] J. Beerten, S. Cole, and R. Belmans, "Modeling of Multi-Terminal VSC HVDC Systems With Distributed DC Voltage Control," *Power Systems, IEEE Transactions on,* vol. 29, pp. 34-42, 2014.

[6] National Grid, "Offshore Development Information Statement " *Company Report,* 2010.

[7] M. M. C. Merlin, T. C. Green, P. D. Mitcheson, D. R. Trainer, R. Critchley, W. Crookes, and F. Hassan, "The Alternate Arm Converter: A New Hybrid Multilevel Converter With DC-Fault Blocking Capability," *Power Delivery, IEEE Transactions on,* vol. 29, pp. 310-317, 2014.

[8] A. Antonopoulos, L. Angquist, and H. P. Nee, "On dynamics and voltage control of the Modular Multilevel Converter," in *Power Electronics and Applications, 2009. EPE '09. 13th European Conference on*, 2009, pp. 1-10.

[9] K. Friedrich, "Modern HVDC Plus application of VSC in Modular Multilevel Converter Topology," *IEEE International Symposium on Industrial Electronics, Bari,* pp. 3807 - 3810 2010.

[10] B. Jacobson, P. Karlsson, G. Asplund, L. Harnefors, and T. Jonsson, "VSC-HVDC Transmission with Cascaded Two-Level Converters," *Cigre Paris Conference,* 2010.

[11] R. Marquardt, A. Lesnicar, and J. Hildinger, "Modulares Stromrichterkonzept für Netzkupplungsanwendung bei hohen Spannungen bei hohen Spannungen," *ETG-Fachbericht,* vol. 88, pp. 155-161, 2002.

[12] T. Qingrui, X. Zheng, and X. Lie, "Reduced Switching-Frequency Modulation and Circulating Current Suppression for Modular Multilevel Converters," *Power Delivery, IEEE Transactions on,* vol. 26, pp. 2009-2017, 2011.
[13] J. Dorn, H. Huang, and D. Retzmann, "Novel Voltage-Sourced Converters for HVDC and FACTS Applications," *Cigre Osaka Conference,* 2007.
[14] H. Saad, S. Dennetie, J. Mahseredjian, P. Delarue, X. Guillaud, J. Peralta, and S. Nguefeu, "Modular Multilevel Converter Models for Electromagnetic Transients," *Power Delivery, IEEE Transactions on,* vol. 29, pp. 1481-1489, 2014.
[15] U. N. Gnanarathna, A. M. Gole, and R. P. Jayasinghe, "Efficient Modeling of Modular Multilevel HVDC Converters (MMC) on Electromagnetic Transient Simulation Programs," *Power Delivery, IEEE Transactions on,* vol. 26, pp. 316-324, 2011.
[16] J. Xu, C. Zhao, W. Liu, and C. Guo, "Accelerated Model of Modular Multilevel Converters in PSCAD/EMTDC," *Power Delivery, IEEE Transactions on,* vol. 28, pp. 129-136, 2013.
[17] H. Saad, J. Peralta, S. Dennetiere, J. Mahseredjian, J. Jatskevich, J. A. Martinez, A. Davoudi, M. Saeedifard, V. Sood, X. Wang, J. Cano, and A. Mehrizi-Sani, "Dynamic Averaged and Simplified Models for MMC-Based HVDC Transmission Systems," *Power Delivery, IEEE Transactions on,* vol. 28, pp. 1723-1730, 2013.
[18] A. Beddard, M. Barnes, and R. Preece, "Comparison of Detailed Modeling Techniques for MMC Employed on VSC-HVDC Schemes," *Power Delivery, IEEE Transactions on,* vol. PP, pp. 1-11, 2014.
[19] ABB, "Its time to connect," *Company Report,* 2008.
[20] National Grid, "2010 Offshore Development Information Statement Appendices," *Company Report,* 2010.
[21] T. Worzyk, *Submarine Power Cables and Their Design Elements*: Springer, 2009.
[22] G. J. Anders, *Rating of Electric Power Cables*: IEEE Press, 1997.
[23] ABB, "XLPE Land Cable Systems User's Guide Revision 5," *Technical guide,* 2010.
[24] A. Beddard and M. Barnes, "HVDC cable modelling for VSC-HVDC applications," in *PES General Meeting | Conference & Exposition, 2014 IEEE*, 2014, pp. 1-5.
[25] S. Maruyama, N. Ishii, M. Shimada, S. Kojima2, H. Tanaka3, M. Asano, T. Yamanaka, and S. Kawakami, "Development of a 500-kV DC XLPE Cable System," *Furukawa Review, No. 25,* 2004.
[26] M. Mohammadi, M. Avendano-Mora, M. Barnes, and J. Y. Chan, "A study on Fault Ride-Through of VSC-connected offshore wind farms," in *Power and Energy Society General Meeting (PES), 2013 IEEE*, 2013, pp. 1-5.
[27] Y. Jiang-Häfner and R. Ottersten, "HVDC with Voltage Source Converters – A Desirable Solution for Connecting Renewable Energies," *Large scale integration of wind power into power systems,* 2010.
[28] L. Livermore, "Integration of Offshore Wind Farms Through High Voltage Direct Current Networks," *Cardiff Univeristy, PhD Thesis,* 2013.
[29] J. Hafner and B. Jacobson, "Proactive Hybrid HVDC Breakers - A key innovation for reliable HVDC grids," *Cigre Bologna Conference,* pp. 1-9, September 2011.
[30] M. Mohaddes, "Hybrid DC Circuit Breaking Device," Patent publication No: WO 2013/093066, Filed: December 2012, Published June 2013.
[31] Alstom Grid, "Alstom confirms research findings, done with RTE, in high-voltage DC circuit-breaker technology," *Press Release,* 24/1/14.
[32] K. Friedrich, "Modern HVDC PLUS application of VSC in Modular Multilevel Converter topology," in *Industrial Electronics (ISIE), 2010 IEEE International Symposium on*, 2010, pp. 3807-3810.
[33] PSCAD, "PSCAD User's Guide," vol. 4.2.1, 2010.
[34] Alstom Grid, *HVDC - Connecting to the future*: Published by Alstom Grid, 2010.
[35] J. Grainger and W. Stevenson, *Power Systems Analysis*: McGraw-Hill, 1994.
[36] L. Ting, M. Barnes, and M. Ozakturk, "Doubly-fed induction generator wind turbine modelling for detailed electromagnetic system studies," *Renewable Power Generation, IET,* vol. 7, pp. 180-189, 2013.
[37] S. K. Chaudhary, R. Teodorescu, P. Rodriguez, and P. C. Kjar, "Chopper controlled resistors in VSC-HVDC transmission for WPP with full-scale converters," in *Conference on Sustainable Alternative Energy* 2009, pp. 1-8.
[38] L. Zeni, I. Margaris, A. D. Hansen, P. E. Sorensen, and P. C. Kjaer, "Generic models of wind turbine generators for advanced applications in a VSC-based offshore HVDC network," in *AC and DC Power Transmission (ACDC 2012), 10th IET International Conference on*, 2012, pp. 1-6.
[39] U. N. Gnanarathna, S. K. Chaudhary, A. M. Gole, and R. Teodorescu, "Modular multi-level converter based HVDC system for grid connection of offshore wind power plant," in *IET ACDC, London*, 2010, pp. 1-5.
[40] A. Lesnicar and R. Marquardt, "An innovative modular multilevel converter topology suitable for a wide power range," in *Power Tech Conference Proceedings, 2003 IEEE Bologna*, 2003, p. 6 pp. Vol.3.
[41] T. Qingrui and X. Zheng, "Impact of Sampling Frequency on Harmonic Distortion for Modular Multilevel Converter," *Power Delivery, IEEE Transactions on,* vol. 26, pp. 298-306, 2011.
[42] J. Peralta, H. Saad, S. Dennetiere, J. Mahseredjian, and S. Nguefeu, "Detailed and Averaged Models for a 401-Level MMC HVDC System," *Power Delivery, IEEE Transactions on,* vol. 27, pp. 1501-1508, 2012.
[43] M. Saeedifard and R. Iravani, "Dynamic Performance of a Modular Multilevel Back-to-Back HVDC System," *Power Delivery, IEEE Transactions on,* vol. 25, pp. 2903-2912, 2010.
[44] N. Bottrell and T. C. Green, "Comparison of Current-Limiting Strategies During Fault Ride-Through of Inverters to Prevent Latch-Up and Wind-Up," *Power Electronics, IEEE Transactions on,* vol. 29, pp. 3786-3797, 2014.
[45] L. Jun, O. Gomis-Bellmunt, J. Ekanayake, and N. Jenkins, "Control of multi-terminal VSC-HVDC transmission for offshore wind power," in *Power Electronics and Applications, 2009. EPE '09. 13th European Conference on*, 2009, pp. 1-10.
[46] Cigre WG B4-52, "HVDC Grid Feasibility Study," *WG Brochure,* 2013.
[47] A. Yazdani and R. Iravani, *Voltage-Sourced Converters in Power Systems*: Wiley 2010.